# Macrobicyclic d-Metal Tris-dioximates Obtained by Cross-linking with p-Block Elements

## Part I. Template Synthesis and Properties of Macrobicyclic Boron-containing Iron(II) Dioximates

YAN Z. VOLOSHIN*, NINA A. KOSTROMINA and ALEXANDER Y. NAZARENKO

*Institute of General and Inorganic Chemistry (Ukrainian SSR Academy of Sciences), 252680 Kiev 142 (U.S.S.R.)*

(Recieved October 9, 1989)

### Abstract

The synthesis and characterization of a number of new boron-containing macrobicyclic iron(II) complexes of the general composition $FeD_3(BR)_2$, where $D^{2-}$ = dioxime anion; R = OH, F, alkyl, alkoxyl, are reported. Infrared, visible, ($^1H$, $^{13}C$, $^{11}B$) NMR and Mössbauer spectra were examined.

The molecular structure of the macrobicyclic complexes was proved by Mössbauer spectroscopy data. The complexes show the geometry of a distorted trigonal prism with different distortion angles in the range 20–30°.

The 'macrocyclic' effects manifested themselves by a decrease in *IS* value in Mössbauer spectra, increase in Debye temperature and molar extinction coefficient and reduction in the width of charge transfer band due to a decrease in the non-rigidity of the complex molecule.

### Introduction

Clathrochelates, macrobicyclic ligand systems that completely encapsulate a metal ion, are known for a number of metals. But only iron(II) clathrochelate complexes (I) based on various dioxime molecules are formed under soft conditions with a high yield. Numerous examples of iron(II) macrobicyclic complexes have been recently reported [1–7]. Several compounds of this group were studied by electrochemical methods [4]. Only tentative information about the geometrical structure of one macrobicyclic iron complex, $FeDm_3(BR)_2$, has been published [1–3]. A few complexes have been studied using Mössbauer [7], PMR [5, 7] and multinuclear NMR [4, 7] spectroscopy.

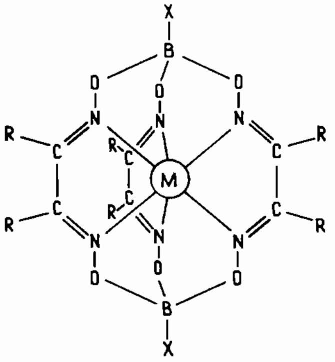

I

In order to systematically study the effect of the dioxime molecule structure as well as of peripheral substituent groups on the structure and spectra of macrocyclic iron(II) complexes, we chose to study a number of known macrobicyclic dioximates and synthesized several new complexes. Infrared and electron spectroscopy, X-ray phase and X-ray diffraction analysis, Mössbauer spectroscopy and multinuclear ($^1H$, $^{13}C$, $^{11}B$) NMR spectroscopy were used.

### Experimental Materials and Apparatus

The reagents used, analytical grade $FeSO_4·7H_2O$, $H_3BO_3$, $Na_2B_4O_7·10H_2O$, $BF_3·(C_2H_5)_2O$, $B(CH_3)_3·NH_3$, phenylglyoxime, dimethylglyoxime, α-benzyldioxime, α-furyldioxime, nioxime and organic reagent grade solvents were obtained commercially. The remaining dioximes shown in Fig. 1 were synthesized and purified by the method reported in ref. 8.

Most of the boron-containing macrobicyclic iron(II) dioximates possess a high oxidation resistance, therefore the synthetic operations were carried out in air. The compounds obtained contain no iron(III) admixtures, which is evidenced by the absence of signals in the ESR spectra of solid samples.

Infrared spectra of solid samples (KBr and CsI tablets) in the range 200–4000 $cm^{-1}$ were recorded on a Pye Unicam SP3-300 spectrophotometer. The assignment of some bands was performed using isotopic substituted compounds. Electron absorption spectra (of solutions in chloroform, dioxane and water) and reflections of solid samples within

---

*Author to whom correspondence should be addressed.

0020-1693/90/$3.50

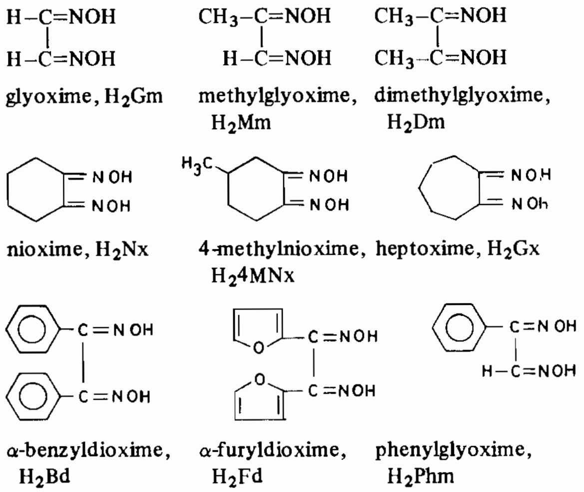

Fig. 1. Starting α-dioximes ($H_2D$) and their designations.

11 000–50 000 $cm^{-1}$ were recorded on a Specord M-40 spectrophotometer. NMR ($^1H$, $^{13}C\{H\}$, $^{11}B$) spectra of solutions in DMSO-$D_6$ and $CDCl_3$ were obtained on a CXP-200 Bruker FT-spectrometer. Mössbauer spectra were obtained on a YGRS-4M spectrometer with a $^{57}Co$ source in the chromium matrix at 80–300 K relative to sodium nitroprusside. For X-ray phase analysis a DRON-3M diffractometer (Cu Kα radiation) was used.

### *Synthesis of Boron-containing Iron(II) Dioximates*

The $FeNx_3(BOH)_2 \cdot 6H_2O$ compound was synthesized by pouring together concentrated aqueous solutions of nioxime, boric acid and $FeSO_4 \cdot 7H_2O$, heated to 80–90 °C, the molar ratio of the ingredients being 3:2:1. The residue precipitated during 10 min in the course of cooling and was filtered off. In the recrystallization of $FeNx_3(BOH)_2 \cdot 6H_2O$, yellowish-orange $FeNx_3(BOH)_2$ crystals were produced from the acetonitrile–water (1:1) mixture by adding one drop of $CF_3COOH$*, and in the recrystallization from dry acetonitrile, dark red $FeNx_3(BOH)_2 \cdot CH_3CN$ crystals were separated. From X-ray phase analysis data it was found that the compounds $FeNx_3(BOH)_2 \cdot 6H_2O$, $FeNx_3(BOH)_2$ and $FeNx_3(BOH)_2 \cdot CH_3CN$ have different crystal structures.

The compounds of composition $FeNx_3(BOR)$, where R is $CH_3$, $C_2H_5$, n-$C_4H_9$, were prepared by heating nioxime, boric acid and $FeCl_2 \cdot 4H_2O$ in the appropriate alcohol in a 3:2:1 molar ratio, followed by driving off a part of the solvent and recrystallizing the product from acetonitrile. The $FeNx_3(BOC_6H_5)_2$ complex was produced by the esterification of the $FeNx(BOH)_2$ complex in molten phenol at 120 °C. The $FeNx_3(BF)_2$, $Fe(4MNx)_3(BF)_2$, $FeGx_3(BF)_2$, $FeNx_3(BCH_3)_2$, $Fe(4MNx)_3(BCH_3)_2$ and $FeGx_3(BCH_3)_2$ compounds were prepared by heating dioxime and $FeCl_2 \cdot 4H_2O$ in butanol or methanol, respectively, with a molar ratio of 3:1, followed by adding a large excess of $BF_3 \cdot (C_2H_5)_2O$ or $B(CH_3)_3 \cdot NH_3$. The precipitated product was recrystallized from acetonitrile or methylene chloride, washed with ethyl ester and dried over $CaCl_2$.

The nioxime series compounds were also prepared by the interaction of $Fe(H_2Nx)_3X_2$ complexes, where X is $\frac{1}{2}SO_4^{2-}$, $NO_3^-$, $Cl^-$, synthesized by the procedure described in ref. 9, with $BF_3 \cdot (C_2H_5)_2O$ in butanol and with $H_3BO_3$ in alcohol or water by heating. The isolated compounds are identical to those prepared by the above method, as confirmed by the results of electron and infrared spectroscopy.

The synthesis of the $Fe(4MNx)_3(BOH)_2$ and $FeGx_3(BOH)_2$ compounds was carried out by pouring together concentrated aqueous solutions of boric acid, the corresponding dioxime and $FeSO_4 \cdot 7H_2O$ heated to 80–90 °C, the molar ratio of the ingredients being 2:3:1. The solution was stirred for 10–15 min, while maintaining the initial temperature, and a saturated aqueous $Na_2B_4O_7 \cdot 10H_2O$ was added dropwise until the pH was 5. Heating and stirring were continued for another 20 min, after which the solution was allowed to stand at room temperature for 1 h. The precipitated residue was recrystallized from hot acetonitrile and dried in vacuum over $CaCl_2$. Template synthesis in dilute aqueous solutions under the same conditions but without heating and recrystallization gives comparatively large $FeGx_3(BOH)_2 \cdot 3H_2O$ crystals.

Compounds of the composition $Fe(4MNx)_3(BOR)_2$, where R is iso-$C_3H_7$, *sec*-$C_4H_9$, n-$C_4H_9$, and $FeGx_3(BOR)_2$, where R is $CH_3$, n-$C_4H_9$, were prepared by heating dioxime, boric acid and $FeCl_2 \cdot 4H_2O$ in a 3:2:1 molar ratio for 15 min at reflux in the appropriate alcohol, followed by the addition of $Na_2B_4O_7 \cdot 10H_2O$. The resulting alcohol solution was evaporated to dryness in vacuum, and the complex was extracted with acetonitrile. After the evaporation of acetonitrile, the oily residue was dissolved in benzene, and the product was isolated in the solid state by precipitation using a threefold excess of hexane. In the case of the lower alcohols ($CH_3OH$, $C_2H_5OH$), compounds of the composition $Fe(4MNx)_3(BOR)_2$ in the solid state for 4-methylnioxime could not be isolated.

The synthesis of the boron fluoride complexes of composition $FeD_3(BF)_2$, where $D^{2-}$ is $H_2Gm$, $H_2Mm$, $H_2Phm$, $H_2Fd$ and $H_2Bd$ dioxime anions, was carried out by the following two methods.

*Method 1.* $FeCl_2 \cdot 4H_2O$ was added to the solution of the corresponding dioxime in a minimum amount of hot butanol in a 3:1 molar ratio, after which the mixture was heated with stirring for 5 min; then a considerable excess of $BF_3 \cdot (C_2H_5)_2O$ was added.

---

*The synthesis of this complex was described in ref. 3.

The residue precipitated during cooling was recrystallized from acetonitrile. In the case of asymmetric dioximes ($H_2Mm$, $H_2Phm$), no solid complex is formed when $BF_3 \cdot (C_2H_5)_2O$ is added. To isolate the complex formed, a threefold volume of benzene or ester was added to its butanol solution, after which the complex was isolated in the solid state by adding a fivefold volume of hexane.

*Method 2.* When bis-dioximates of the composition $Fe(HD)_2Py_2$ interact with $BF_3 \cdot (C_2H_5)_2O$ in hot butanol, boron fluoride $FeD_3(BF)_2$ complexes are formed, where $D^{2-}$ is $H_2Gm$, $H_2Mm$, $H_2Dm$, $H_2Bd$, $H_2Fd$, $H_2Nx$, $H_2Phm$ and $H_2Gm$ dioxime anions. The identity of the solid products to those prepared by method 1 was confirmed by electron and infrared spectroscopy data.

The above reactions may be presented in the following form:

$$Fe^{2+} + 3H_2D + 2B(OH)_3 + 2ROH \xrightarrow{ROH, t^0} FeD_3(BOR)_2 + 2H^+ + 6H_2O$$

$$Fe^{2+} + 3H_2D + 6BF_3 \xrightarrow[\text{excess of } BF_3 \cdot (C_2H_5)_2O]{n\text{-}C_4H_9OH} FeD_3(BF)_2 + 6H^+ + 4BF_4^-$$

$$Fe(H_2D)_3{}^{2+} + 2BR_3 \longrightarrow FeD_3(BR)_2 + 4HR + 2H^+$$

$$3Fe(HD)_2Py_2 + 12BF_3 \xrightarrow{n\text{-}C_4H_9OH} 2FeD_3(BF)_2 + 6H\rangle + 8BF_4^-$$

The individual nature of the isolated complexes was confirmed by elementary and X-ray phase analyses. The synthesized substances are stable-in-air compounds intensively coloured from yellow to red–violet and readily soluble in polar organic solvents.

## Results and Discussion

The infrared spectra of the synthesized compounds (Table 1) confirm their macrobicyclic nature nature: in all the spectra there are no wide characterisitic bands for $\nu$(OH) vibrations in the range 2600–3200 $cm^{-1}$ [9], which belong to the vibrations of free oxime groups. In addition, a number of intense bands are revealed, which are typical of the boron atom in a tetrahedral environment. The C=N bond stretching vibration bands at 1600 $cm^{-1}$ are shifted and considerably strengthened; the value of the shift is small for alicyclic dioximes and much higher for acyclic dioximates, which indicates a variation in the ligand structure during complexing. The C=N bond stretching vibration band is observed for all dioximates close to 1580 $cm^{-1}$, which indicates a similar structure for the coordination polyhedron in all the synthesized compounds. Only in glyoximate, is this band observed at 1559 $cm^{-1}$, which correlates with the data of X-ray diffraction analysis: the length of the C=N bond in glyoxime is 1.28 Å and in dimethylglyoxime it is 1.25 Å.

Stretching vibrations of the C–H bonds in cycloalkane rings, methyl and phenyl substituents in dioximes at 3000 $cm^{-1}$ are insensitive to complexing; only in the case of glyoximate is the shift of the narrow absorption band for the C–H bond 90 $cm^{-1}$. The most sensitive to coordination in the case of alicyclic dioximes were bonding vibrations of cycloalkane ring methylene groups, whose absorption bands shifted by 15–40 $cm^{-1}$ toward the long-wave region. Only in the case of boron–methyl complexes is the shift small (1–18 $cm^{-1}$), which is associated with the electron-donor effect of the substituent at the boron atom, whose characteristic bonding vibrations are observed close to 1310 $cm^{-1}$.

Electron absorption spectra of complexes in the visible and near UV regions contain an absorption band having a maximum in the 19 000–23 000 $cm^{-1}$ range; the same band is also observed in the reflection spectra of solid samples. On breaking down into Gaussian components, a more intensive band ($\epsilon$ = (2–3) $\times 10^4$ $mol^{-1}$ l $cm^{-1}$) and a weaker (3 $\times 10^3$ $mol^{-1}$ l $cm^{-1}$) band were distinguished. The long-wave band is interpreted as a metal–ligand ($M \rightarrow L\pi^*$) charge transfer band (CTB); in the UV spectral region of the complexes, intraligand transitions are observed, which are shifted relative to the absorption spectrum of the starting dioxime.

The position of the CTB in a complex correlates with that of the absorption band for a free ligand in the UV region (Fig. 2). This supports the suggestion of a metal–ligand charge transfer: the position of the upper occupied orbital in Fe(II) is, in a first approximation, independent of the nature of the substituent in the oxime molecule. At the same time, a decrease in the energy of the lower unoccupied ligand orbital (to which a decrease in electron transition energy in a ligand molecule corresponds) results in a decrease of the energy difference between the occupied orbital in Fe and the unoccupied orbital in the ligand; this causes a shift of the CTB toward the long-wave region.

The molar absorptivity of the CTB in macrobicyclic complexes is considerably (by 1.5–2 fold) higher than in their non-macrocyclic analogues. At the same time, the line half-width in the case of the latter is noticeably higher (Figs. 3 and 4), i.e. the line integral intensity remains unchanged when macrobicyclic complexes are formed. The decrease in CTB line half-width in macrobicyclic complexes may be associated with a decrease in the dynamic non–rigidity of the complex molecules during encapsulation.

TABLE 1. Characteristics of electronic and IR spectra for the synthesized iron(II) dioximates

| Compound | $\nu_{max} \times 10^{-3}$ (cm$^{-1}$) | $\epsilon \times 10^{-4}$ (mol$^{-1}$ l cm$^{-1}$) | $\nu$(C=N) | $\nu$(N–O) (cm$^{-1}$) | $\nu$(B–O) |
|---|---|---|---|---|---|
| $H_2Nx$ | | | 1575, 1645 | 1260 | |
| $FeNx_3(BF)_2$ | 22.5 | 1.84 | 1584 | 1225 | 1190 |
| $FeNx_3(BOH)_2 \cdot 6H_2O$ | 22.3 | 1.80 | 1577 | 1228 | 1190 |
| $FeNx_3(BOH)_2$ | 22.3 | 1.80 | 1577 | 1228 | 1199 |
| $FeNx_3(BOH)_2 \cdot CH_3CN$ | 22.3 | 1.75 | 1580 | 1233 | 1198 |
| $FeNx_3(BOCH_3)_2$ | 22.3 | 1.74 | 1582 | 1233 | 1198 |
| $FeNx_3(BOC_2H_5)_2$ | 22.4 | 1.74 | 1581 | 1233 | 1194 |
| $FeNx_3(BOn\text{-}C_4H_9)_2$ | 22.4 | 1.73 | 1582 | 1233 | 1194 |
| $FeNx_3(BOC_6H_5)_2$ | 22.4 | 1.60 | 1580 | 1233 | 1190 |
| $FeNx_3(BCH_3)_2$ | 22.2 | 1.66 | 1576 | 1230 | 1104 |
| $H_24MNx$ | | | 1580, 1647, 1658 | 1277, 1280 | |
| $Fe(4MNx)_3(BF)_2$ | 22.2 | 2.00 | 1599 | 1228, 1260 | 1190 |
| $Fe(4MNx)_3(BOH)_2$ | 22.2 | 1.80 | 1591 | 1235 | 1195 |
| $Fe(4MNx)_3(BOiso\text{-}C_3H_7)_2$ | 22.2 | 1.68 | 1595 | 1230, 1260 | 1195 |
| $Fe(4MNx)_3(BOsec\text{-}C_4H_9)_2$ | 22.3 | 1.54 | 1591 | 1230, 1260 | 1194 |
| $Fe(4MNx)_3(BOn\text{-}C_4H_9)_2$ | 22.3 | 1.52 | 1596 | 1228, 1243 | 1193 |
| $Fe(4MNx)_3(BCH_3)_2$ | 22.2 | 1.88 | 1579 | 1246, 1281 | 1103 |
| $H_2Gx$ | | | 1602, 1634 | 1247 | |
| $FeGx_3(BF)_2$ | 22.4 | 2.02 | 1569 | 1254 | 1176 |
| $FeGx_3(BOH)_2$ | 22.3 | 2.03 | 1576 | 1278 | 1189 |
| $FeGx_3(BOCH_3)_2$ | 22.4 | 1.70 | 1577 | 1268 | 1178 |
| $FeGx_3(BOn\text{-}C_4H_9)_2$ | 22.4 | 1.52 | 1573 | 1278 | 1170 |
| $FeGx_3(BCH_3)_2$ | 22.1 | 1.31 | 1540, 1570 | 1250 | 1108 |
| $FeGm_3(BF)_2$ | 23.0 | 1.66 | 1559 | 1231 | 1207 |
| $FeMm_3(BF)_2$ | 22.8 | 1.62 | 1585 | 1239 | 1217 |
| $FeDm_3(BF)_2$ | 22.7 | 1.70 | 1585 | 1238 | 1194 |
| $FeFd_3(BF)_2$ | 19.5 | 3.60 | 1584 | 1230 | 1210 |
| $FeBd_3(BF)_2$ | 20.7 | 3.13 | 1582 | 1250 | 1212 |
| $FePhm_3(BF)_2$ | 21.4 | 2.52 | 1580 | 1256 | 1217 |

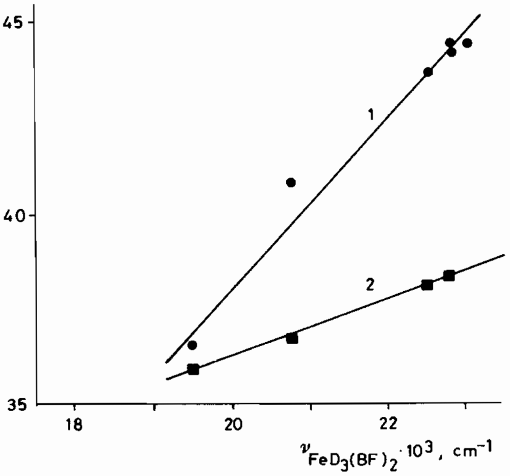

Fig. 2. Correlation dependence of $\nu_{max}$ of CTB in $FeD_3(BF)_2$ complexes on $\nu_{max}$ of the intraligand transfer band in the $H_2D$ (1) molecule and $HD^-$ ion (2).

To verify this assumption, temperature dependences of NGR parameters (Figs. 5 and 6) were obtained for the $FeNx_3(BOH)_2$, $Fe(4MNx)_3(BOH)_2$ and $FeGx_3(BOH)_2$ clathrochelate complexes as well as for their non-macrocyclic analogue, $Fe(H_2Nx)_3SO_4$. The results obtained are given in Table 2. The temperature shift of Mössbauer lines, $\Delta V$, in the high temperature or classic limit is described by the following equation [10]

$$\Delta V(T) = \Delta V_o - \frac{3E_\gamma}{4Mc^2} k\theta_D \mathrm{cth}\left(\frac{\theta_D}{2T}\right)$$

where $\theta_D$ is the Debye temperature.

This allows one to easily determine the value of the latter for each of the complexes using the data from Table 2.

In a harmonic interatomic-bond-forces-in-crystal approximation, the probability of absorption without energy loss by recoil (probability of the Mössbauer effect) is given by [10]

$$f' = \exp\left\{-\frac{\langle x^2 \rangle \times 4\pi^2}{\lambda}\right\}$$

where $\lambda$ is the wave length of the $\gamma$-quantum; $\langle x^2 \rangle$ is the mean square of the Mössbauer nucleus vibration amplitude.

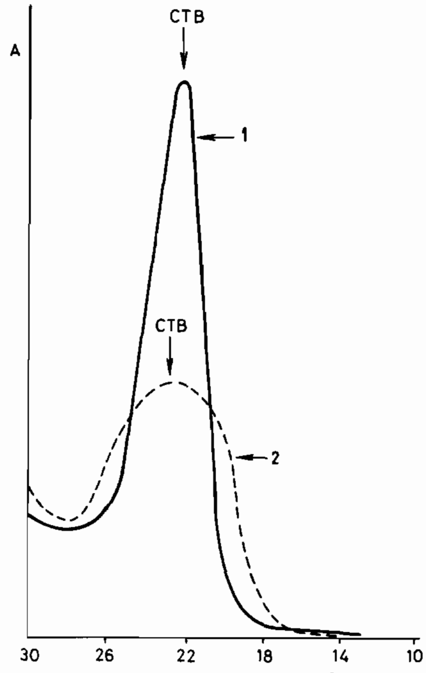

Fig. 3. Fragments of electronic absorption spectra for $FeNx_3(BOH)_2$ (1) and $Fe(H_2Nx)_3SO_4$ (2) complex solutions at equal concentrations.

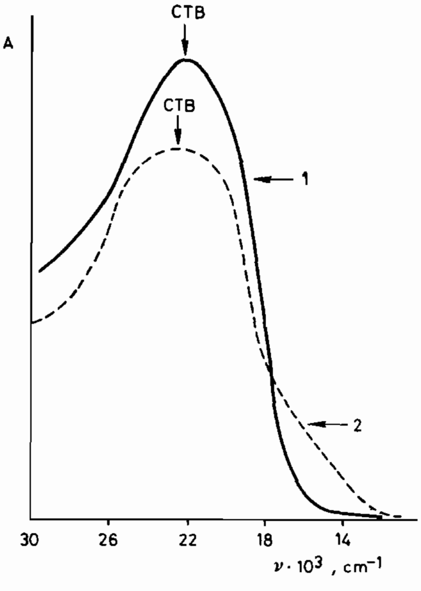

Fig. 4. Fragments of electronic reflection spectra for the $FeNx_3(BOH)_2$ (1) and $Fe(H_2Nx)_3SO_4$ (2) complexes.

On the other hand, in terms of the Debye model for a solid body, an expression for $f'$ was obtained depending on the absorbing crystal temperature [10]

$$f' = \exp\left\{-\frac{6R}{k\theta_D}\left(\frac{T}{\theta_D} + \frac{\theta_D}{36T}\right)\right\}$$

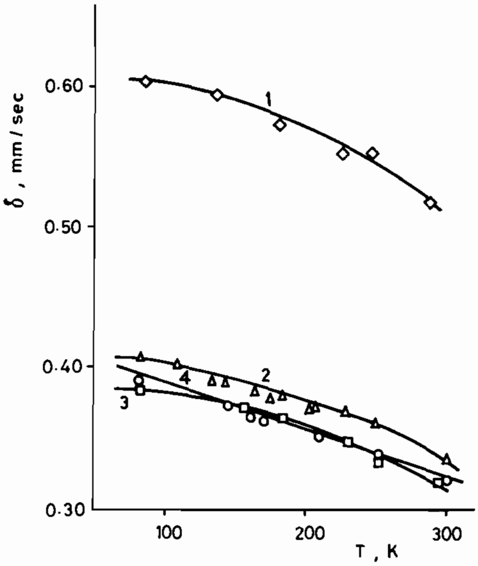

Fig. 5. Isomeric shift in the Mössbauer spectra for the $Fe(H_2Nx)_3SO_4$ (1), $FeGx_3(BOH)_2$ (2), $Fe(4MNx)_3(BOH)_2$ (3) and $FeNx_3(BOH)_2$ (4) complexes as a function of temperature.

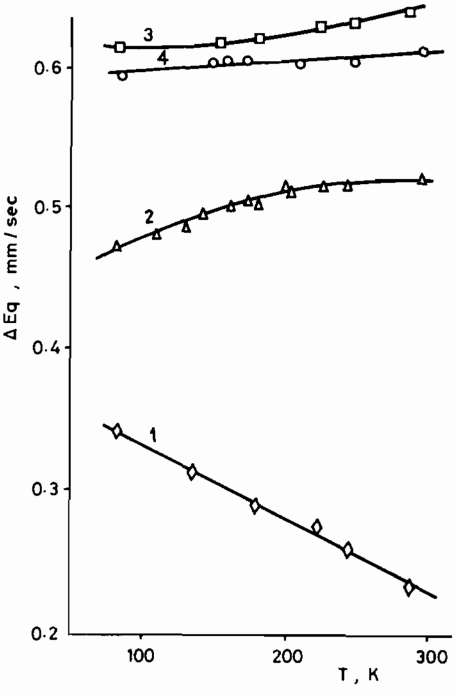

Fig. 6. Quadrupole splitting in the Mössbauer spectra for the $Fe(H_2Nx)_3SO_4$ (1), $FeGx_3(BOH)_2$ (2), $Fe(4MNx)_3(BOH)_2$ (3) and $FeNx_3(BOH)_2$ (4) complexes as a function of temperature.

where $R$ is the recoil energy of the Mössbauer nucleus with allowance for $\theta_D$ and $T$ values. The $\theta_D/36T$ ratio may be neglected in this particular case as compared with the $T/\theta_D$ one, and the equation will take the form

TABLE 2. Parameter values of Mössbauer spectra for complexes at different temperatures[a]

| | | | | | | | |
|---|---|---|---|---|---|---|---|
| $[Fe(H_2Nx)_3]SO_4$ $\theta_D = 470 \pm 30$ K | | | | | | | |
| *T* (K) | 291 | 246 | 225 | 180 | 135 | 86 | |
| *IS* (mm/s) | 0.512 | 0.550 | 0.547 | 0.575 | 0.592 | 0.602 | |
| *QS* (mm/s) | 0.233 | 0.260 | 0.276 | 0.291 | 0.314 | 0.344 | |
| $FeNx_3(BOH)_2$ $\theta_D = 600 \pm 30$ K | | | | | | | |
| *T* (K) | 300 | 249 | 210 | 174 | 159 | 150 | 83 |
| *IS* (mm/s) | 0.317 | 0.334 | 0.347 | 0.359 | 0.361 | 0.368 | 0.385 |
| *QS* (mm/s) | 0.616 | 0.602 | 0.600 | 0.605 | 0.605 | 0.606 | 0.596 |
| $Fe(4MNx)_3(BOH)_2$ $\theta_D = 600 \pm 30$ K | | | | | | | |
| *T* (K) | 293 | 252 | 228 | 183 | 155 | 83 | |
| *IS* mm/s) | 0.315 | 0.331 | 0.342 | 0.360 | 0.368 | 0.384 | |
| *QS* (mm/s) | 0.642 | 0.635 | 0.633 | 0.624 | 0.620 | 0.619 | |
| $FeGx_3(BOH)_2$ $\theta_D = 600 \pm 30$ K | | | | | | | |
| *T* (K) | 300 | 248 | 228 | 206 | 203 | 184 | |
| *IS* (mm/s) | 0.330 | 0.358 | 0.364 | 0.368 | 0.369 | 0.378 | |
| *QS* (mm/s) | 0.520 | 0.515 | 0.514 | 0.510 | 0.516 | 0.502 | |
| *T* (K) | 176 | 163 | 143 | 133 | 109 | 83 | |
| *IS* (mm/s) | 0.375 | 0.380 | 0.387 | 0.388 | 0.400 | 0.405 | |
| *QS* (mm/s) | 0.502 | 0.500 | 0.497 | 0.482 | 0.481 | 0.474 | |

[a] ± 0.005 mm/s.

$$f' = \exp\left\{-\frac{6RT}{k\theta_D^2}\right\}$$

By comparing these two expressions for the probability of the Mössbauer effect, the following equation

$$\langle x^2 \rangle = \frac{6RT\lambda}{4\pi^2\theta_D^2}$$

which connects the mean square of the Mössbauer nucleus vibration amplitude to the squared Debye temperature is easy to obtain. Thus, the higher value of the Debye temperature in macrobicyclic complexes, as against their non-macrocyclic analogues, unambiguously indicates a decrease in the dynamic non-rigidity of complex molecules during encapsulation.

Mössbauer parameters of synthesized iron clathrochelates are listed in Table 3. For the purpose of comparison isomeric shifts (*IS*) and quadrupole splittings (*QS*) for a number of known Fe(II) compounds are also given. It should be noted that $FeD_3(BR)_2$ complexes, like other iron(II) dioximates, are diamagnetic, and our results are in satisfactory (with allowance for experimental conditions) agreement with the data obtained by other authors. The *IS* values for a series of complexes having the same ligand but different cross-linking fragments depend slightly on the nature of the substituent at the boron atom and maybe, therefore, considered to be typical of the given oxime.

To estimate the determining factors of contributions made by various parameters to the variation of *IS* values, calculations of expected *IS*s for nioximate and phenanthrolinate complexes were carried out in terms of the principle of additivity of partial *IS* in pseudo- and octahedral low-spin iron(II) complexes [15]. When using partial *IS* values of ligands it was taken into consideration that the partial *IS* of the molecular species $H_2Nx$ is 0.02 mm/s higher than that for the $HNx^-$ ion. Comparison between the calculated and experimental *IS* values demonstrates that in the case of non-macrocyclic tris-complexes, a practically perfect agreement of these values is observed. When a macrobicyclic ligand is formed within the coordination sphere of iron, the experimental *IS* value is essentially lower than the calculated one.

It has been noted that the *IS* value for iron(II) complexes decreases in the order Phen > bipy > $NO_2^-$ > $H_2Nx$ > $CN^-$ > NO and correlates with an increase in the ligand field. This fact suggests that the presence of intraligand binding boron-containing fragments causes an increase in the ligand field force, i.e. a 'macrocyclic effect' takes place, accompanied in particular by an increase in the s-electron density on the iron(II) atom, and hence by a decrease in the *IS* value.

The *QS* values for macrobicyclic dioximates with aliphatic substituents proved to be, as can be seen from Table 3, noticeably higher than those observed for pseudo- or octahedral complexes with a similar

TABLE 3. Parameters of Mössbauer spectra for some iron(II) complexes ($T$ = 300 K)

| Compound | *IS* (mm/s) | *IS* estimate (mm/s) | *QS* (mm/s) | Distortion angle estimate (°) |
|---|---|---|---|---|
| $FeGm_3(BF)_2$ | 0.31 | | 0.56 | 21–23 |
| $FeMm_3(BF)_2$ | 0.32 | | 0.70 | 20–22 |
| $FeDm_3(BF)_2$ | 0.31 | | 0.90 | 18–20 |
| $FePhm_3(BF)_2$ | 0.29 | | 0.44 | 22–24 |
| $FeFd_3(BF)_2$ | 0.35 | | 0.14 | 30–32 |
| $FeBd_3(BF)_2$ | 0.32 | | 0.25 | 27–30 |
| $Fe(4MNx)_3(BF)_2$ | 0.31 | | 0.69 | 20–22 |
| $Fe(4MNx)_3(BOH)_2$ | 0.32 | | 0.63 | 20–22 |
| $Fe(4MNx)_3(BOn\text{-}C_4H_9)_2$ | 0.34 | | 0.61 | 20–22 |
| $Fe(4MNx)_3(BCH_3)_2$ | 0.34 | | 0.60 | 20–22 |
| $FeGx_3(BF)_2$ | 0.29 | | 0.58 | 20–22 |
| $FeGx_3(BOH)_2 \cdot 3H_2O$ | 0.32 | | 0.47 | $23.5^b$ |
| $FeGx_3(BOCH_3)_2$ | 0.33 | | 0.49 | 22–24 |
| $FeGx_3(BOn\text{-}C_4H_9)_2$ | 0.34 | | 0.46 | 22–24 |
| $FeGx_3(BCH_3)_2$ | 0.35 | | 0.34 | 26–28 |
| $FeNx_3(BCH_3)_2$ | 0.33 | 0.40 | 0.60 | 20–22 |
| $FeNx_3(BF)_2$ | 0.33 | 0.40 | 0.68 | 20–22 |
| $FeNx_3(BOH)_2$ | 0.32 | 0.40 | 0.62 | 20–22 |
| $[FePhen_3]C_2O_4$ [11] | 0.57 | 0.58 | −0.29 | |
| $Fe(HNx)_2Py_2$ [12] | 0.46 | 0.46 | 1.76 | |
| $[Fe(H_2Nx)_3]Cl_2$ [13] | 0.52 | 0.52 | 0.28 | |
| $Fe(HNx)_2(H_2Nx)$ [13] | 0.44 | 0.44 | 0.61 | |
| $FeL(BF)^{+a}$ [14] | | | +0.95 | |

[a] $L^{3-}$ :

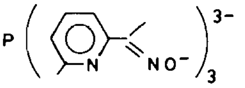

X-ray diffraction analysis data, see ref. 18.

donor environment of iron(II) (e.g. tris-nioximate or phenanthrolinate), although they are lower than the values given for complexes with a tetragonal symmetry.

Analysis of the literature and our data allows one to suppose that a distorted trigonal prism structure is realized in $FeD_3(BR)_2$ compounds. The degree of distortion, characterized by the angle of deviation from the ideal prism ($\varphi$), is determined by the ligand nature. It should be noted also that the *QS* value changes its sign in the series of complexes having different degrees of coordination sphere polyhedron distortion (Fig. 7).

In low-spin iron(II) complexes the three lowest d-orbitals are occupied (for octahedral complexes these are $t_{2g}$-orbitals). In the case of trigonal distortion, the $t_{2g}$-level splits into $a_1$ and $e_1$. The value of such a splitting, with allowance for the insignificant contribution of $\pi$-binding, was estimated [16] for tris-diimine complexes. It is known that at $\varphi$ = 60°, tris-diimine complexes have the $D_3$ symmetry instead of $O_h$, which results in the non-zero value of splitting. As the angle $\varphi$ decreases, the splitting decreases down to zero ($\varphi$ = 40–50°), after which an inversion of the levels takes place, and the splitting again increases (Fig. 7). It should be noted that the splitting of $t_{2g}$-levels and the absolute value of *QS* are symbate. The sign of *QS* for tris-phenanthrolinate complexes proved to be negative ($\varphi$ = 56°) and for $FeL(BF)^+$ positive ($\varphi$ = 22°). It follows from the close structures of $FeD_3(BF)_2$ and $FeL(BF)^+$ complexes and positive *QS* values that the measured *QS* values correspond to the angles of rotation of the dioxime groups and are 18–20° for dimethylglyoxime, 20–24° for other aliphatic oximes and 27–32° for benzyl- and furyldioxime. These angles differ only slightly from the values obtained from an X-ray diffraction analysis of the

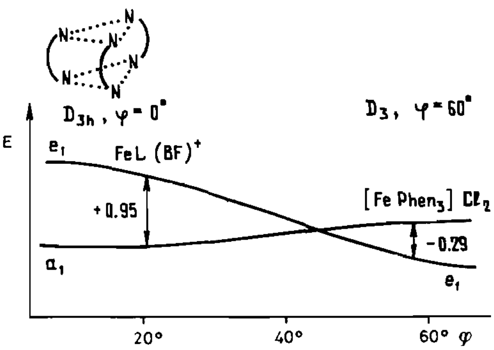

Fig. 7. $t_{2g}$-level splitting value vs. coordination polyhedron distortion angle (0° for trigonal prism).

$CoDm_3(BF)_2$ and $[CoDm_3(BF)_2]BF_4$ complexes of similar compositions (8.6 and 31.2° respectively) [17]. For complexes with the same starting dioxime but different cross-linking fragments, *IS* insignificantly decreases in the series of substituents at the boron atom, $F \leqslant OH < On\text{-}C_4H_9 < CH_3$, which formally corresponds to an increase in ligand field force in this series; the increase in quadrupole splitting indicates the structure of boron fluoride complexes to be closer to a trigonal prism. Replacement of fluorine by larger and less electronegative groups leads to a decrease in packing density in the crystalline structure, an increase in interatomic distances, a decrease in ligand field force and to the coordination polyhedron becoming closer to a octahedron, which is optimal for the $d^6$ configuration. The abnormally low *QS* value in the case of the $FeGx_3(BCH_3)_2$ complex may be caused by steric hindrances arising through the interaction of a bulk methyl substituent at the boron atom with the α-methylene group of a dioxime fragment.

The value of quadrupole splitting decreases with temperature for clathrochelate complexes, while its absolute value increases for the $Fe(H_2Nx)_3SO_4$ non-macrocyclic complex. However, taking into account the data of its X-ray structure analysis and using Fig. 7, it is possible to assume a negative sign for the *QS* value in this complex. In other words, the *QS* value decreases with temperature both in macrocyclic and non-macrocyclic complexes, which indicates an increase in the distortion angle in the trigonal-prismatic structure with temperature.

In PMR spectra of $FeD_3(BR)_2$ compounds (Table 4), the value of the chemical shift of protons in the aliphatic groups of the complexes increases by 0.1–0.5 ppm as against a corresponding dioxime, indicating a general redistribution of the electron density in the system of ligand bonds through a charge transfer from ligand to metal and a change in ligand conformation.

The signals of α-methylene group protons are the most sensitive to complexing in the case of alicyclic groups, which correlates with IR spectroscopic data. The proton lines of the dioxime groups in nioximates and heptoximates are somewhat broadened singlets. Such a shape of lines in most sterically unhindered cycloalkanes with a large ring size indicates their dynamic nature: because of the easy variation in the cycloalkane ring conformation at room temperature, spin–spin interactions between different methylene groups are not observed. Introduction of a methyl substituent into the cyclohexane ring hinders conformational transitions, and spin–spin interaction is distinctly revealed in the PMR spectra of 4-methylnioxime and its complexes.

The PMR spectra of 4-methylnioxime and its complexes are very close to one another, which indicates a small variation in oxime conformation

TABLE 4. Parameters of ($^1H$, $^{13}C$, $^{11}B$) NMR spectra for boron fluoride clathrochelate complexes of iron(II) and corresponding dioximes

| Compound | $^{13}C$ relative to TMS (ppm) | | | $^1H$ relative to TMS (ppm) | | $^{11}B$ relative to $NaB(C_6H_5)_4$ | |
|---|---|---|---|---|---|---|---|
| | $\delta(^{H}{>}C{=}NO-)$ | $\delta(^{R}{>}C{=}NO-)$ | $\delta(R-)$ | $\delta(^{H}{>}C{=}NO-)$ | $\delta(R-)$ | δ (ppm) | $J_{B-F}$ (Hz) |
| $FeGm_3(BF)_2$ | 143.10 | | | 8.27 | | 10.30 | 15.7 |
| $H_2Gm$ | 145.31 | | | 7.77 | | | |
| $FeMm_3(BF)_2$ | 145.41 | 152.29 | 13.41 | 7.18 | 2.36 | 10.33 | 14.7 |
| | | | | | | 10.38 | 14.7 |
| $H_2Mm$ | 147.29 | 151.73 | 9.11 | 7.65 | 1.92 | | |
| $FeDm_3(BF)_2$ | | 153.15 | 13.12 | | 2.26 | 10.38 | 14.2 |
| $H_2Dm$ | | 152.98 | 9.22 | | 1.97 | | |
| $FeBd_3(BF)_2$ | | 156.62 | 127.81 | | 7.37 | 10.24 | 11.7 |
| | | | 129.17 | | | | |
| | | | 129.98 | | | | |
| | | | 130.87 | | | | |
| $H_2Bd$ | | 155.19 | 127.48 | | 7.37 | | |
| | | | 127.81 | | | | |
| | | | 128.88 | | | | |
| | | | 132.81 | | | | |
| $FePhm_3(BF)_2$ | 147.07 | 151.55 | 128.47 | 8.86 | 7.39 | 10.49 | 15.3 |
| | | | 129.58 | | 7.56 | | |
| | | | 130.79 | | | | |
| $H_2Phm$ | 140.63 | 150.82 | 127.63 | 8.53 | 7.33 | | |
| | | | 128.44 | | 7.54 | | |
| | | | 134.06 | | | | |
| $FeFd_3(BF)_2$ | | | | | | 10.49 | 15.6 |

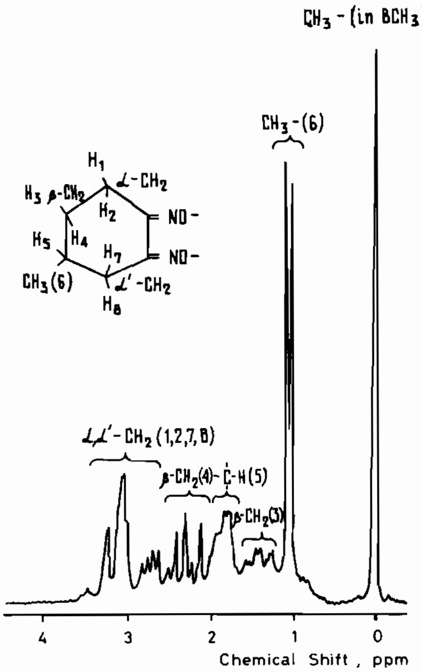

Fig. 8. PMR spectrum for a solution of $Fe(4MNx)_3(BCH_3)_2$ in $CDCl_3$.

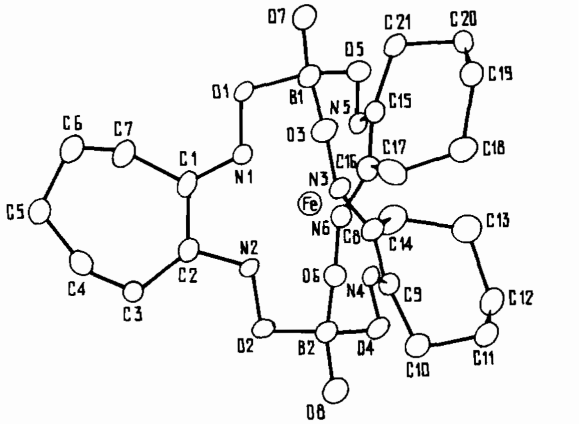

Fig. 9. Molecular structure of the $FeGx_3(BOH)_2 \cdot 3H_2O$ complex.

by complexing. To assign the lines in these spectra, a number of model compounds (cyclohexanone, 4-methylcyclohexanone and their oximes) were studied, and experiments on double resonance (suppression of spin–spin interactions) were carried out, allowing groups of lines to be assigned (Fig. 8).

While in PMR spectra a strong descreening of cycloalkane ring protons is revealed during complexing, the change in effective charge on carbon atoms correlating with the chemical shift value is essentially smaller and even different in sign for α- and β-methylene group carbons in the case of nioximates and 4-methylnioximates according to $^{13}C$ NMR spectroscopic data. Relative shifts caused by the carbon atoms of substituted and non-substituted oxime groups in acyclic dioximates are also different in sign. In the latter case, the parameters of the lines due to the carbon atoms of the substituents change substantially. The reason for this phenomenon could be a change in oxime conformation: acyclic oximes existing in the free state in a *trans*-form acquire a *cis*-configuration during complexing, resulting in an essential (up to 4 ppm) change in the chemical shift value.

The $^{11}B$ NMR spectra of boron fluoride complex solutions show one line, a doublet, which appears through the spin–spin $^{11}B$–$^{19}F$ interaction, which confirms the existence of cross-linking B–F groups in the complexes. The chemical shift value ($\delta NaB(C_6H_5)_4$ = 10–12 ppm) indicates a tetrahedral environment of boron atoms in synthesized complexes, and the small value of $J_{B-F}$ (10–15 Hz) a high symmetry of this environment. In the case of $FeD_3(BR)_2$ complexes, where R ≠ F, a singlet is observed in $^{11}B$ NMR spectra, which has the same chemical shift value and is broadened because of the interaction between boron atoms and substituent protons.

Using the method of kinetically controlled template synthesis from a dilute aqueous solution, single crystals of the $FeGx_3(BOH)_2 \cdot 3H_2O$ complex were obtained (space group *C*2/*c*). Analysis of the crystalline and molecular structures of this complex (Fig. 9) demonstrated [18] that the iron atom is encapsulated by a bulky macrobicyclic ligand and is in a distorted trigonal-prismatic environment formed by six nitrogen atoms. The value of the distortion angle ($\varphi \sim 23.5°$) is close to that estimated from the data of Mössbauer spectroscopy (Table 3). The Fe–N distance in the complex is 1.91 Å, and the cycloheptane ring has a chair conformation.

The comparatively high selectivity of macrobicyclic iron(II) dioximate formation reactions and the stability of these dioximates may be attributed to the favourable action of the main factors affecting the ability of a metal ion to form macrobicyclic clathrochelate compounds.

– Under the effect of a strong field of $D_3$ symmetry, produced by six nitrogen atoms of three dioxime groups, the binding $t_{2g}$-level is completely filled, thereby ensuring a high stability of the electron configuration of the $Fe^{2+}$ ion.

– In terms of the HSAB Pearson principle [19], among all the kinds of donor atoms it is nitrogen atoms that possess the highest affinity for the $Fe^{2+}$ ion, which results in a large energy gain in the formation of compounds whose coordination number is six.

– The conformity between the sizes of the macrobicyclic ligand cavity and the Fe(II) ion can be explained using concepts of physical ionic radii, which depend on the coordination number and ion spin state. According to the data of X-ray diffraction analysis, the M–N distance in such macrobicyclic complexes is *c.* 1.9 Å, which yields (with allowance for the physical radius of nitrogen) an optimum physical radius of the metal of 0.6–0.7 Å. This value is observed in low-spin $Fe^{2+}$ (0.75 Å) and $Co^{3+}$ (0.69 Å) complexes. With the coordination number six, Ni(II), Co(II) and Cu(II) have a larger physical radius, and the macrobicyclic ligand cavity has not enough room for them.

– The presence of conjugated $\pi$-bonds in dioxime and the rigidity of the boron-containing cross-linking fragment result in the relative rigidity of the ligand. Thus, the number of metal ions for which the formation of boron-containing tris-dioximate complexes can occur is sharply restricted.

As a result of the effect of the above factors, in the case of Fe(II) a maximum possible number of cross-links is realized on the boron atom to form a macrobicyclic structure, and the complexes have a higher stability as against their macrocyclic and acyclic analogues. Therefore, $FeD_3(BR)_2$ tris-dioximates can also be obtained through the interaction between the corresponding $Fe(HD)_2Py_2$ and $BR_3$. Cross-linking by the $BR_2$ group to form two-dimensional macrocyclic $Fe(DBR_2)_2$ complexes is not observed in contrast to Ni, Cu and Co compounds. Macrobicyclic Fe(II) complexes are formed most readily by alicyclic dioximes, with a quantitative yield and various boron-containing cross-linking fragments; these dioximes exist only in the *cis*-form, which facilitates the complexation process and increases the stability of the resulting compounds.

The formation of complexes is somewhat more difficult in the case of dimethylglyoxime and $\alpha$-benzyldioxime. For glyoxime, methylglyoxime, phenylglyoxime and $\alpha$-furyldioxime only boron–fluoride complexes were obtained. An attempt to isolate complexes of *o*-benzoquinonedioxime, oxamidoxime and cyclopentanediondioxime failed, which can be explained by their structural peculiarities. In the series of substituents at the boron atom, boron fluoride complexes are formed most readily and with a great amount of dioximes. Boron–alkyl and boron–aryl complexes and (in the case of some dioximes) compounds with the BOR cross-linking group are formed somewhat less readily.

The formation of clathrochelate structures by the encapsulation of d-metal tris-dioximates is characteristic not only of boron-containing compounds. Compounds of other p-block elements, which are Lewis acids, such as tin, germanium(IV), antimony, bismuth, arsenic(III) halides are also efficient encapsulating agents. The results of investigations in this field will be reported in the near future.

## Supplementary Material

A list of elemental analysis data and complete tables of crystallographic data are available from Dr Y. Z. Voloshin on request.

## Acknowledgements

We thank Dr S. I. Tyukhtenko and Dr E. V. Polshin for their assistance in recording NMR and Mössbauer spectra, and Dr S. V. Lindeman and Professor Y. T. Struchkov for the collection of X-ray intensity data.

## References

1 D. R. Boston and N. J. Rose, *J. Am. Chem. Soc., 95* (1973) 4163.

2 S. C. Jackels and N. J. Rose, *Inorg. Chem., 12* (1972) 1232.

3 S. C. Jackels, J. Zektzer and N. J. Rose, *Inorg. Synth., 17* (1978) 139.

4 M. K. Robbins, D. W. Naser, J. L. Heiland and J. J. Grzybowski, *Inorg. Chem., 24* (1985) 3381.

5 A. Y. Nazarenko and Y. Z. Voloshin, *Zh. Neorg. Khim., 29* (1984) 1776.

6 Y. Z. Voloshin, A. Y. Nazarenko and V. V. Trachevskii, *Ukr. Khim. Zh., 51* (1985) 121.

7 E. V. Polshin, V. V. Trachevskii, S. I. Tyukhtenko, A. Y. Nazarenko and Y. Z. Voloshin, *Koord. Khim., 13* (1987) 96.

8 C. V. Banks, D. T. Hooker and J. J. Richard, *J. Organ. Chem., 21* (1956) 547; W. V. Haar, R. C. Voter and C. V. Banks, *J. Organ. Chem., 14* (1949) 836; M. Wittenberg and V. Meyer, *Chem. Ber., 16* (1883) 500; L. Claisen, *Chem. Ber., 20* (1887) 252; V. M. Peshkova, V. M. Savostina and E. K. Ivanova, *Oximy*, Nauka, Moscow, 1977.

9 D. G. Batyr, I. I. Bulgak and L. D. Ozol, *Koord. Khim., 4* (1978) 84.

10 V. I. Goldanskii and R. H. Herber (eds.), *Chemical Applications of Mössbauer Spectroscopy*, Academic Press, New York, 1968.

11 J. F. Duncan and K. F. Mok, *J. Chem. Soc. A*, (1966) 1493.

12 A. V. Ablov, V. I. Goldanskii, R. A. Stukan, K. I. Turta and V. I. Zubarev, *Dokl. AN SSSR, 186* (1969) 850.

13 K. I. Turta, R. A. Stukan, I. I. Bulgak, L. G. Batyr and L. D. Ozol, *Koord. Khim., 4* (1978) 1391.

14 W. M. Reiff, *J. Am. Chem. Soc., 95* (1973) 3048.

15 G. M. Bancroft, M. J. Hays and B. E. Prater, *J. Chem. Soc. A*, (1970) 956.

16 E. Larsen, G. N. La Mar, B. E. Wagner and R. H. Holm, *Inorg. Chem., 12* (1972) 2652.

17 G. A. Zakrewski, C. A. Chilardi and E. C. Lingafelter, *J. Am. Chem. Soc., 93* (1971) 4411.

18 S. V. Lindeman, Y. Z. Voloshin and Y. T. Sruchkov, *Koord. Khim.*, in press.

19 R. G. Pearson, *J. Am. Chem. Soc., 89* (1963) 3533.